J Mater Sci (2010) 45:3096–3101
DOI 10.1007/s10853-010-4317-7

The effect of Ca on the in vitro corrosion performance of biodegradable Mg–Nd–Y–Zr alloy

E. Aghion · G. Levy

Received: 31 December 2009 / Accepted: 10 February 2010 / Published online: 5 March 2010

Abstract The effect of 0.4% Ca on the in vitro corrosion behavior of Mg–1.2% Nd–0.5% Y–0.5% Zr was evaluated in a simulated physiological environment in the form of 0.9% NaCl solution saturated with $Mg(OH)_2$ at ambient temperature and at 37 °C. The microstructure examination was carried out using optical microscopy, scanning electron microscopy, transmission electron microscopy, and X-ray diffraction analysis. The corrosion behavior was evaluated by immersion test, salt spray testing, and potentiodynamic polarization analysis. The stress corrosion behavior was examined using slow strain rate testing analysis in different strain rates. The results obtained have shown that the addition of 0.4% Ca has a beneficial effect on the corrosion resistance of the tested alloy. This was mainly attributed to the effect of calcium, which reduces oxidation in the molten condition and consequently improves the soundness of the obtained casting. Hence, it is believed that the reduction in the extent of inherent casting defects in the alloy containing calcium overcomes the detrimental micro-galvanic effect of the Mg_2Ca phase that was formed in the tested alloy. Contrary to the beneficial effect of calcium on the corrosion performance, the addition of calcium has a damaging effect on the stress corrosion behavior in terms of reduced ultimate tensile strength and ductility. This was mainly due to the embrittlement effect of calcium that was generated by the formation and distribution of Mg_2Ca phase at grain boundaries.

Introduction

The potential of magnesium alloys to serve as a structural material for biodegradable implants is already documented in the literature for use in orthopedic and cardiovascular applications [1–7]. According to Williams [8], the release of elemental magnesium from corroding magnesium alloys should not cause toxicity and may have positive beneficial effects on some structures, including cells in the relevant local tissue. However, the corrosion of magnesium can lead to premature loss of mechanical integrity of the implant [9] and to the formation of excessive hydrogen gas that can cause separation of tissues [10], and in extreme cases gas embolism. Hence, in order to address those two main drawbacks of biodegradable magnesium implants, their corrosion degradation should be controlled and comply with the hydrogen absorption capability of the neighboring tissue.

One of the main tools to address the degradation kinetics of magnesium alloys is controlling their chemical composition [11–13]. Calcium is considered one of the alloying elements that can modify the corrosion resistance of magnesium alloys in a simulated physiological environment (SPE) such as Hank solution, simulated body fluid (SBF), and normal saline (0.9% NaCl solution). According to Kannan and Singh Raman [14], potentiodynamic polarization and electrochemical impedance spectroscopy analysis in SBF carried out on AZ91 and AZ61 magnesium alloys containing 1 wt% Ca showed that calcium addition significantly enhanced the general and pitting corrosion resistance of those alloys. This result was also obtained by Wan et al. [15] while evaluating the corrosion resistance of Mg–0.6% Ca, and by Zhang and Yang [16] on Mg–Zn–Mn–Ca alloy. According to Zhang and Yang, the improved corrosion resistance was attributed to the formation of

---

E. Aghion (✉) · G. Levy
Department of Materials Engineering, Ben-Gurion University of the Negev, P.O. Box 653, Beer-Sheva 84105, Israel
e-mail: egyon@bgu.ac.il

Mg_2Ca phase. Relating to the effect of calcium on the mechanical properties of binary Mg–Ca alloys, Li et al. [17] found that the yield strength (YS), ultimate tensile strength (UTS), and elongation decreased with increasing calcium content. In terms of the effect of calcium on toxicity, Li et al. indicated that cytocompatibility evaluation using L-929 cells revealed that Mg–1% Ca alloy did not introduce toxicity to cells, and the viability of cells for Mg–1% Ca alloy extraction medium was better than that of the control.

The aim of the present study is to evaluate the effect of calcium on the in vitro corrosion performance of biodegradable Mg–1.2% Nd–0.5% Y–0.5% Zr alloy in SPE. The selected alloy was chosen due to the relatively adequate biocompatibility of Neodymium and Yttrium and their beneficial effect on the corrosion behavior and mechanical properties, respectively [18, 19]. The overall motivation of the study was to explore the potential capability of the Mg–Nd–Y–Zr–Ca system to serve as a structural material for a biodegradable implant having adequate degradation kinetics.

Experimental

The chemical composition of the two magnesium alloys tested by the present investigation is shown in Table 1. This includes the composition of the magnesium alloy containing calcium (EW10X04) and that of the base alloy (EW10) without calcium. Both alloys were used in as cast condition and the casting procedure included the following stages: remelting of pure magnesium at 775 °C, addition of pure Zr, Nd, and Y with agitation; melt settling for about 40 min until adequate ladle composition is obtained. Following the remelting and alloying processes, the melted alloy was cast in a steel mold to obtain 8 kg ingots. In the case of the EW10X04 alloy, the previous casting procedure was followed by addition of calcium in the form of master-alloy Mg–30% Ca, with agitation. After adding the calcium, an additional settling time of 30 min was required before final casting of the ingots.

The microstructure characteristics of the tested alloys was obtained by optical microscopy, scanning electron microscopy (SEM) with an energy dispersive spectrometer (JEOL JSM-5600) (EDS), transmission electron microscopy (TEM), and X-ray diffraction analysis using a Rigaku-2100 diffractometer with CuKα wavelength. The X-ray tube parameters were 40 kV/30 mA and the scanning rate was 2°/min.

Table 1 Chemical composition of tested alloys

Alloy	Nd (wt%)	Y (wt%)	Zr (wt%)	Ca (wt%)	Fe (ppm)	Mg (wt%)
EW10X04	1.16	0.48	0.48	0.43	37	Bal
EW10	1.15	0.43	0.46	–	46	Bal

The corrosion performance of the tested alloys was evaluated by immersion test according to ASTM standard G31-72. This test included measurement of hydrogen evolution that is indicative of the corrosion rate [20]. The electrochemical behavior was evaluated by potentiodynamic polarization analysis using a scanning rate of 0.5 V/h, according to ASTM standard G-59-97. The stress corrosion behavior was examined using slow strain rate testing (SSRT) according to ASTM G129-00 standard. The diameter of the SSRT test specimen was 3.80 mm, while the gauge length was 25.4 mm. The SPE used by the above corrosion tests was 0.9% NaCl solution saturated with $Mg(OH)_2$ at ambient temperature and at 37 °C. The saturation with $Mg(OH)_2$ aimed at eliminating the effect of the corrosion products $(OH)^-$ on the corrosiveness of the solution [21]. The outdoor corrosion behavior of the tested alloys was evaluated by salt spray testing (3.5% NaCl solution) using an Angelantoni DCTC 600P corrosion test cabinet according to ASTM B117 standard.

Results and discussion

The typical microstructure of EW10 and EW10X04 alloys by optical microscopy is shown in Fig. 1. This revealed that the average grain size of EW10 alloy was 43.7 ± 0.2 μm while that of EW10X04 alloy containing calcium was only 37.6 ± 3.1 μm. The refining effect of calcium obtained with the EW10X04 alloy was in accord with the findings of Zhang and Yang [16], who tested the effect of 0.3–1.0% calcium on an Mg–Zn–Mn system. An enlarged view of the microstructure of EW10X04 alloy and spot chemical analysis of the grain interior and at the tri-pole junction of grain boundaries obtained by SEM and EDS analysis are shown in Fig. 2. These clearly highlight the significant enrichment of Nd and Ca at grain boundaries that is indicative of their limited solubility in α magnesium matrix.

The phase composition of the tested alloys was obtained by X-ray diffraction analysis as shown in Fig. 3. This indicated that the main precipitate phase in both alloys was $Mg_{41}Nd_5$. However, the calcium-containing alloy included an additional Mg_2Ca phase. The domination of the main precipitate phase $Mg_{41}Nd_5$ at grain boundaries was also obtained by the TEM analysis as shown in Fig. 4. According to this analysis, the crystal structure of $Mg_{41}Nd_5$ was HCP with lattice parameters: $a = 14.66$ Å and $c = 10.00$ Å. The mechanical properties of the tested alloys at room temperature are shown in Table 2. While the YS of the two alloys was relatively close, significant

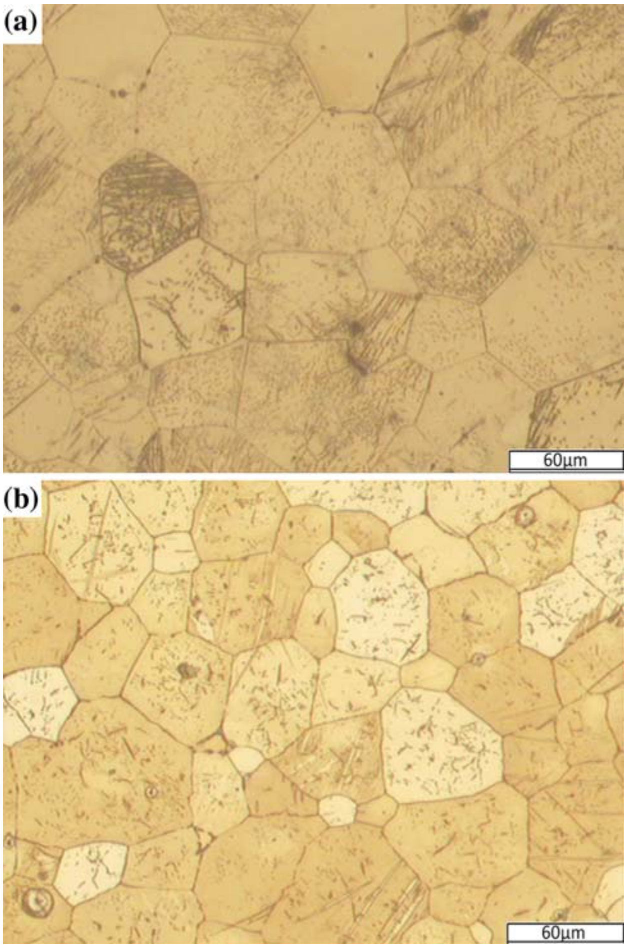

Fig. 1 Typical microstructure obtained by optical microscopy (×200). **a** EW10 alloy, **b** EW10X04 alloy containing calcium

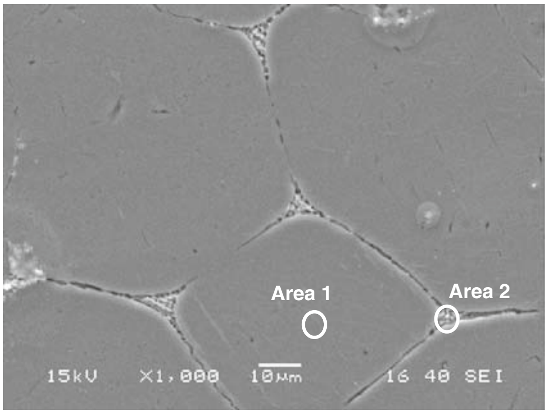

	Mg(%wt)	Nd(%wt)	Y(%wt)	Zr(%wt)	Ca(%wt)
Area 1	97.8±0.35	1.25±0.14	0.5±0.09	0.18±0.1	0.3±0.04
Area 2	82.2±0.28	14.5±0.35	0.76±0.09	0.14±0.1	2.3±0.09

Fig. 2 Microstructure of EK10X04 alloy and corresponding chemical composition of the grain interior and at tri-pole junction of grain boundaries as obtain by SEM and EDS analysis

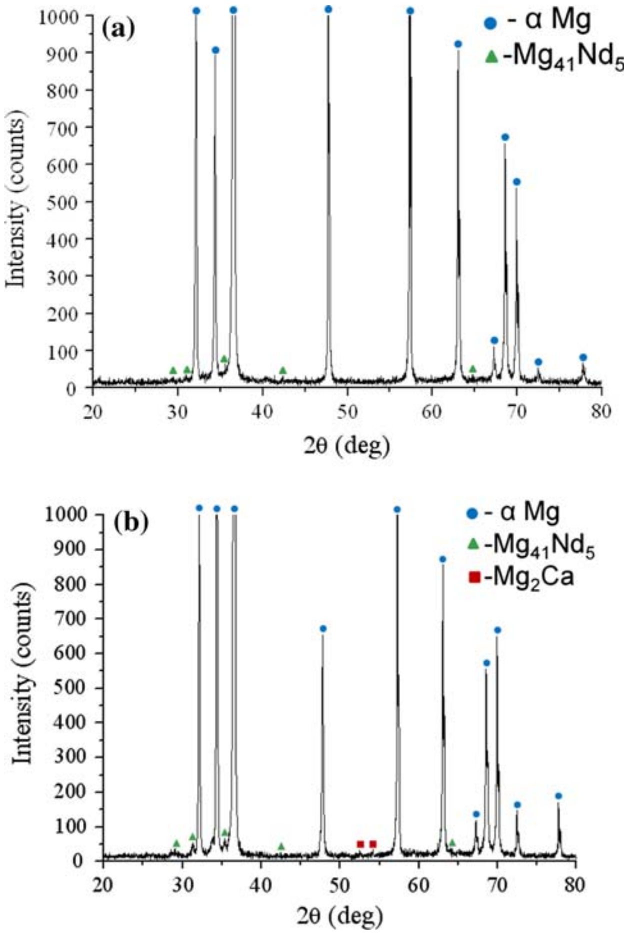

Fig. 3 X-ray diffraction analysis of **a** EW10 alloy, **b** EW10X04 alloy

differences were obtained in the UTS and elongation. The calcium-containing alloy had much lower UTS and was relatively more brittle. Those results are in line with the observation of Li et al. [17], who tested the effect of calcium on the mechanical properties of binary Mg–Ca alloys. In both cases, it is believed that the significant reduction in UTS and elongation is mainly attributed to the formation and distribution of Mg_2Ca phase at grain boundaries.

The in vitro corrosion performance of the tested alloys obtained by measurement of hydrogen evolution during immersion tests in 0.9% NaCl solution and by salt spray testing in terms of weight loss is shown in Figs. 5 and 6, respectively. The significantly higher corrosion rates obtained by the salt spray testing were due to the higher concentration of NaCl solution (3.5 vs. 0.9% in the immersion test). Both tests clearly indicate that the corrosion resistance of the magnesium alloy containing calcium (EW10X04) was improved compared to that of the base alloy (EW10). This result was also supported by the potentiodynamic polarization analysis as shown in Fig. 7 and Table 3. The fact that the corrosion resistance of magnesium alloys can be improved by relatively small additions

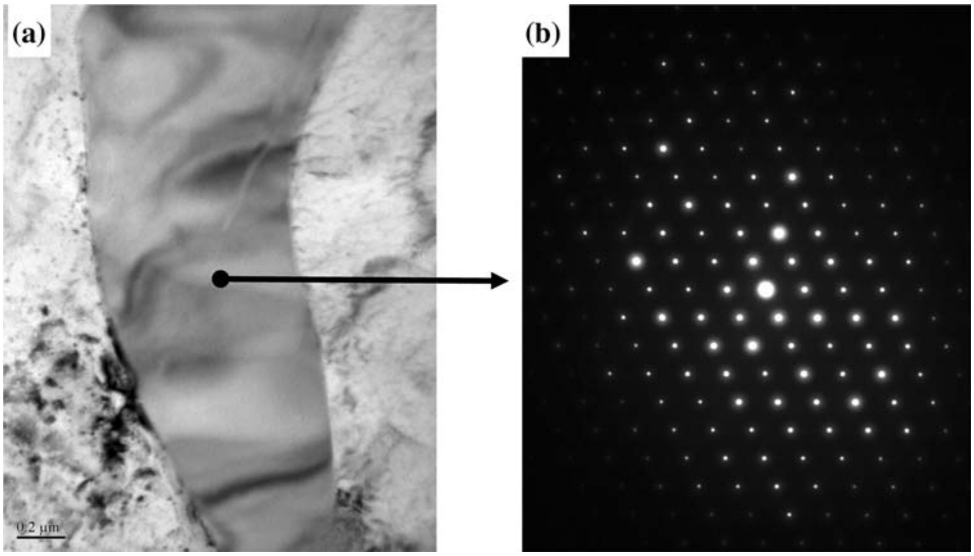

Fig. 4 TEM analysis of EK10 alloy. **a** Microstructure of grain boundaries showing the presence of a dark phase between two grains; **b** diffraction pattern of the dark phase indicating the presence of $Mg_{41}Nd_5$ precipitate

Table 2 The mechanical properties of EW10 and EW10X04 alloys at ambient temperature

Alloy	YS (MPa)	UTS (MPa)	Elongation (%)
EW10X04	74 ± 5	135 ± 4	5 ± 1
EW10	77 ± 4	175 ± 11	12 ± 3

of calcium was also demonstrated by Wan et al. [15] on pure Mg with 0.6% Ca and by Zhang and Yang [16] on Mg–Zn–Mn alloy with up to 1% calcium. However, at relatively larger quantities of calcium, usually above 1%, the corrosion resistance of magnesium alloys is reduced [15, 22]. This was explained by the micro-galvanic corrosion between the magnesium matrix with a corrosion potential of $-2.37\ V_{SHE}$ and the Mg_2Ca phase with a corrosion potential of $-1.54\ V_{SHE}$ [22]. The controversy relating to the effect of the Mg_2Ca phase on corrosion resistance is not clear, as it is evident that the existence of that phase at relatively small amounts of calcium does not result in reduction of the corrosion resistance. According to our understanding, the improved corrosion resistance of magnesium alloys with a small amount of Ca (up to 1%) should not be related to the formation of Mg_2Ca phase. It is believed that since addition of small amounts of calcium reduces oxidation in the molten condition [23], it consequently may also improve the soundness of the obtained casting. In addition, according to Ghalli et al. [24], calcium initially dissolved in α-Mg improves the overall corrosion properties of the alloy by lowering the α-Mg activity. Hence, the improvement in the corrosion resistance of the tested alloy containing calcium (EW10X04) can be attributed to the reduction of inherent casting defects and to the beneficial effect of Ca on the activity of α-Mg. Both effects simultaneously overcome the detrimental micro-galvanic effect of the Mg_2Ca phase.

The stress corrosion behavior of the tested alloys obtained by the SSRT in 0.9% NaCl solution in term of UTS and elongation versus strain rate is shown in Figs. 8 and 9, respectively. This revealed that the UTS of the alloy containing Ca (EW10X04) was significantly reduced at lower strain rate ($10^{-8}\ s^{-1}$) compared to that of the base alloy without Ca. In addition, the strain rate sensitivity factor (m) fitted to the UTS curve equation ($\sigma_{UTS} = C \cdot \dot{\varepsilon}^{m}$) of the alloy containing Ca was 0.2091, while that of the base alloy was only 0.0216, indicating that the stress corrosion sensitivity [25] of the alloy containing Ca was significantly greater. In terms of elongation versus strain rate, the reduced ductility of the alloy containing Ca was maintained in all the tested strain rates compared to the base alloy.

In general, as the stress corrosion mechanism of magnesium alloys can be divided into two main stages: incubation and cracking [25], where the incubation phase

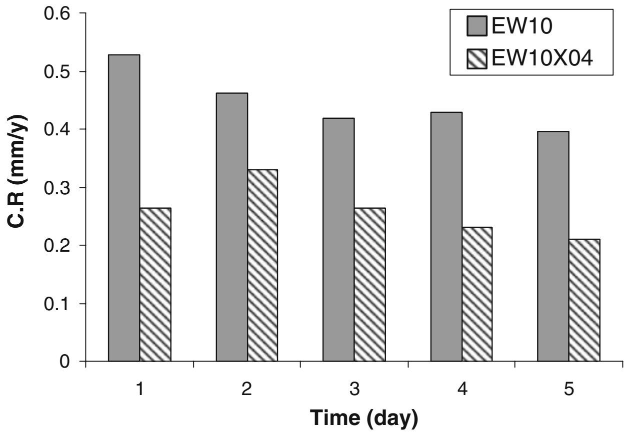

Fig. 5 Corrosion rate calculated from hydrogen evolution obtained during immersion tests of EW10 and EW10X04 alloys in 0.9% NaCl solution at 37 °C

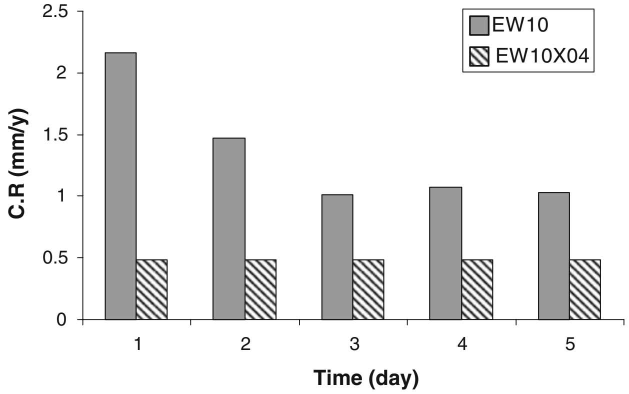

Fig. 6 Corrosion rate calculated from salt spray testing of EW10 and EW10X04 alloys according to ASTM B117 standard

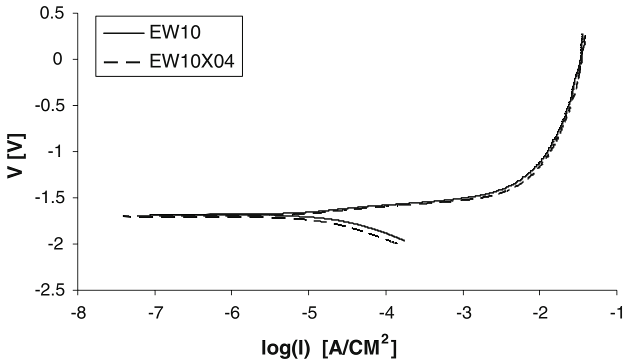

Fig. 7 Potentiodynamic polarization curves obtained in 0.9% NaCl solution at ambient temperature

Table 3 Measurements obtained from potentiodynamic polarization tests in 0.9% NaCl solution at ambient temperature

	EW10X04	EW10
I_{CORR} (μA)	8.04	14.6
E_{CORR} (V)	−1.65	−1.68
CR (mm/year)	0.18	0.3

Corrosion rate (CR) was calculated from Tafel extrapolation

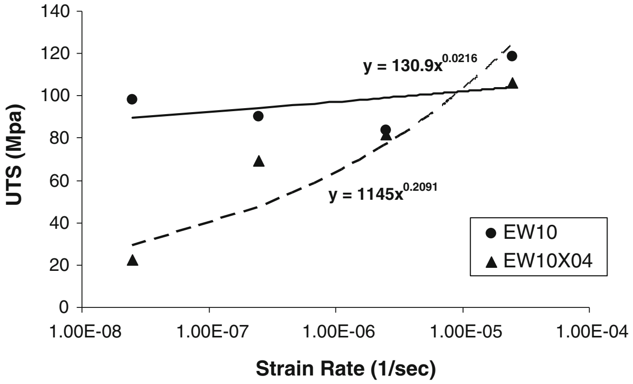

Fig. 8 The effect of strain rate on UTS as obtained from the SSRT tests in 0.9% NaCl solution at ambient temperature

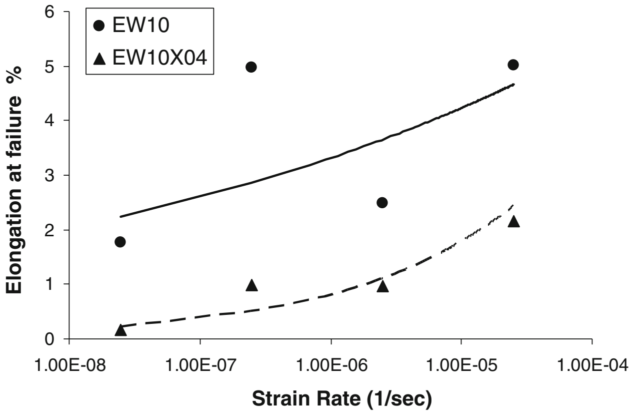

Fig. 9 The effect of strain rate on elongation as obtained from the SSRT tests in 0.9% NaCl solution at ambient temperature

relates to the initial dissolution of magnesium according to the following reaction:

$$Mg + 2H_2O \rightarrow Mg(OH)_2 + H_{2(g)}.$$

It is believed that the main different between the alloy with Ca and the one without Ca relates to the cracking phase. According to this understanding the hydrogen produced during the incubation stage reduces the cohesive strength of the magnesium matrix, which generates typical conditions for hydrogen embrittlement and subsequent cracking under external applied load [26, 27]. Hence, it is believed that the reduced stress corrosion resistance of the alloy containing Ca is mainly due to the inherent embrittlement of this alloy as shown in Table 2 in terms of relative UTS and elongation. The inherent embrittlement of this alloy significantly reduces the alloy resistance to cracking, which practically results in a dramatic drop in the stress corrosion resistance in terms of its mechanical properties at reduced SSRT strain rates.

Conclusion

The in vitro corrosion resistance of Mg–1.2% Nd–0.5% Y–0.5% Zr alloy with addition of 0.4% Ca was improved compared to the base alloy that did not contain calcium. Contrary to the positive effect of Ca on corrosion resistance, Ca addition has a detrimental effect on the stress corrosion resistance in terms of UTS and elongation versus strain rate as obtained by the SSRT analysis.

Acknowledgements The authors would like to thank Ms. Meital Hillel from Ben-Gurion University for her assistance in the experimental work.

References

1. Aghion E, Arnon A, Atar D, Segal G (2007) US Patent No. PCT/IL 2007/000520
2. Brar HS, Platt MO, Sarntinoranont M, Martin PI, Manuel MV (2009) JOM 61:31
3. Gu X, Zheng Y, Cheng Y, Zhong S, Xi T (2009) Biomaterials 30:484
4. Muller WD, Nascimento ML, Zeddies M, Corsico M, Gassa LM, Lorenzo de Mele MA (2007) Mater Res 10:5
5. Witte F, Fischer J, Nellesen J, Crostack HA, Kaese V, Pisch A, Beckmann F, Windhagen H (2006) Biomaterials 27:1013
6. Heublein B, Rohde R, Kaese V, Niemeyer M, Hartung W, Haverich A (2003) Heart 89:651
7. Song G, Song S (2007) Adv Eng Mater 9:298
8. Williams D (2006) Med Dev 17:9
9. Erinc M, Sillekens WH, Mannens R, Werkhoven RJ (2009) In: Nyberg EA, Agnew SR, Neelameggham NR, Pekguleryuz MO (eds) Magnesium technology 2009. TMS 2009, Annual meeting & exhibition, San Francisco, California, USA, 15–19 February 2009
10. Staiger MP, Pietak AM, Huadmai J, Dias G (2006) Biomaterials 27:1728
11. Song G (2007) Corros Sci 49:1696
12. Aghion E, Gueta Y, Moscovitch N, Bronfin B (2008) J Mater Sci 43:4870. doi:10.1007/s10853-008-2708-9
13. Liu N, Wang J, Wa Y, Wang L (2008) J Mater Sci 43:2550. doi:10.1007/s10853-008-2447-y
14. Kannan MB, Singh Raman RK (2008) Biomaterials 29:2306
15. Wan Y, Xiong G, Luo H, He F, Huang Y, Zhou X (2008) Mater Des 29:2034
16. Zhang E, Yang L (2008) Mater Sci Eng A 497:111
17. Li Z, Gu X, Lou S, Zheng Y (2008) Biomaterials 29:1329
18. Stroganov GB, Savitski EM, Tikhov NM, Terekhova VF, Volkov MV, Sivash KM, Borodkin VS (1972) US Patent No. 3687135
19. Quach NC, Uggowitzer PJ, Schmutz P (2008) Chimie 11:1043
20. Song G, Atrens A (2003) Adv Eng Mater 5:837
21. Aghion E, Lulu N (2009) J Mater Sci 44:4279. doi:10.1007/s10853-009-3634-1
22. Kim WC, Kim JG, Lee JY, Seok HK (2008) Mater Lett 62:4146
23. Avedesian MM, Baker H (1999) Magnesium and magnesium alloys (ASM specialty handbook). ASM International, Materials Park, OH
24. Ghali E, Dietzelw W, Kainer KU (2004) J Mater Eng Perform 13(1):7
25. Arnon A, Aghion E (2008) Adv Eng Mater 10:742
26. Song RG, Blawert C, Dietzel W, Atrens A (2005) Mater Sci Eng A 399:308
27. Kannan MB, Dietzel W, Singh Raman RK, Lyon P (2007) Scr Mater 57:579